Int. J. Nanosci. Nanotechnol., Vol. 10, No. 3, Sept. 2014, pp. 153-162

Calculation of Heat Transfer Coefficient of MWCNT-TiO_2 Nanofluid in Plate Heat Exchanger

M. A. Safi[1], A. Ghozatloo[1,2*], A. A. Hamidi[3], M. Shariaty-Niassar[1]

1- Transport Phenomena and Nanotechnology Laboratory, Department of Chemical Engineering, College of Eng., University of Tehran, Tehran, I. R. Iran

2- Faculty member of Research Institute of Petroleum Industry (RIPI), West blvd. Azadi Sport Complex,Tehran, I.R.Iran

3- Department of Chemical Engineering, College of Eng., University of Tehran, Tehran, I. R. Iran

(*) Corresponding author: ghozatlooa@ripi.ir

(Received: 30 Dec. 2013 and accepted: 18 July 2014)

Abstract:

The objective of the present study is the synthesis of MWCNT-TiO_2 hybrid nanostructures by solvothermal synthesis method with $TiCl_4$ as precursor. The heat transfer enhancement due to the use of MWCNT-TiO_2 nanofluid was investigated. As-prepared hybrid materials were characterized by X-ray diffraction (XRD) and scanning electron microscopy (SEM). The results showed that MWCNTs were uniformly decorated with anatase nanocrystals. The heat transfer performance of the plate heat exchanger (PHE) was investigated using MWCNT-TiO_2 nanofluid at various volume flow rates, a wide range of concentrations and inlet temperatures. The performance is discussed in terms of heat transfer coefficient ratio. The results showed that the heat transfer coefficient of the nanofluid was more than that of the base fluid (Distilled Water). The heat transfer coefficient was enhanced with increasing the nanofluid concentration from 0.02 to 0.08 wt.% and volume flow rate from 2 to 3.5 LPM. Conversely, the heat transfer coefficient decreased with increasing the nanofluid inlet temperature from 36 to 60°C.

Keywords: *Nanofluids, Plate heat exchanger, Heat transfer, Hybrid*

1. INTRODUCTION

The plate heat exchangers (PHEs) are compact and efficient, widely used in many engineering applications because of their high thermal efficiency, compactness, usefulness in varying loads, flexibility and ease of sanitation. To take care of the growing demand for energy density, heat transfer capacity needs to be increased and this can be attained by the use of a fluid with better transport properties. Innovative heat transfer fluids suspended by nanometer-sized solid particles are called ‘nanofluids’ which was coined by Choi in 1995 [1]. These fluids include metal oxides, chemically stable metals and several allotropes of carbon with thermal conductivities typically an order-of-magnitude higher than those of the base fluids and with sizes significantly smaller than 100 nm[2].

The heat transfer enhancement when using nanofluids may be affected by several mechanisms such as Brownian motion, sedimentation, dispersion of the suspended particles, thermophoresis, diffusiophoresis, layering at the solid/liquid interface and ballistic phonon transport. It should be noted that the increase in thermal conductivity might be offset by the increase in viscosity and decreased the effective specific heat of nanofluid.

However, various experiments showed significant heat transfer enhancement with little penalty of pressure drop in heat exchanger applications [3-6].
Carbon nanotubes (CNTs) have drawn extensive attention owing to their promising applications in various fields. One of the most important applications is employing CNTs as scaffolds of various oxides like TiO_2 [7] to construct functional carbon-based hybrids or composites. Many methods including self-assembly, sol–gel coating [8], hydrothermal, solvothermal, and liquid/vapor phase deposition have recently been developed to prepare this kind of hybrids. Most of these methods are generally employed in aqueous reactive systems [7] where pristine hydrophobic CNTs require to be pre-oxidized in strong acids into their hydrophilic forms containing –OH and –COOH. However, the oxidization usually causes uncontrollable damage to the structure of CNTs [8], undesired surface defects and shortening of CNTs, which exerts adverse effects on the conductivity and mechanical properties of pristine CNTs. Therefore, it becomes important to develop new strategies for preparing uniform hybrids with pristine CNTs as starting supports [9].
The objective of the present study is the synthesis of MWCNT-TiO_2 hybrid by solvothermal method and investigating the heat transfer enhancement due to the use of MWCNT-TiO_2 nanofluid in a PHE. Experiments were conducted in a wide range of concentrations (0.02, 0.04, 0.06 and 0.08 wt.%), temperatures (36, 44, 52 and 60°C) and volume flow rates (2, 2.5, 3 and 3.5 LPM).

2. EXPERIMENTAL PROCEDURES

2.1. Materials

The multiwall carbon nanotube was purchased from Research Institute of Petroleum Industry (RIPI). Sulfuric acid (H_2SO_4), Nitric acid (HNO_3), titanium chloride ($TiCl_4$) and Ethanol were purchased from Merck KGaA (Darmstadt, Germany).

2.2. Functionalization of Multiwall Carbon Nanotube

The raw-MWCNTs were sonicated for 3 h at 60°C in an ultrasonic bath with a (v/v, 3:1) mixture of concentrated H_2SO_4 and HNO_3 to introduce oxygen containing functional groups on the raw-MWCNT surface. The load of MWCNTs was 1 g for 80 mL of the blended acid solution. Then the mixture was diluted by distilled water, and it was filtered and washed repeatedly till the washing showed no acidity. The clean MWCNTs were dried in the oven at 60°C for 12 hours [10]. The reaction scheme for the treatment of CNTs using Acid treatment is shown in Figure 1.

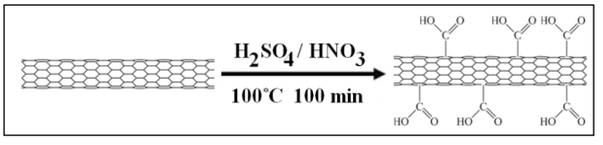

Figure 1: *Scheme reaction for Acid treatment of CNTs*

2.3. Synthesis of MWCNT-TiO_2 hybrid

The MWCNT-TiO_2 hybrid nanostructures were prepared from titanium chloride by solvothermal method. Briefly, 0.5 mL $TiCl_4$ (4.55 mmol) was slowly dropped into 40 mL ethanol and stirred magnetically to provide a completely transparent yellow solution. Desired amounts of MWCNT were dissolved, placed in the ultrasonic bath for 45 min and dispersed in the solution. Then it was transferred to a Teflon-lined, stainless autoclave and stored at 120°C for 24 h, until it turned into gray or dark precipitate. The precipitate was separated by centrifugation and washed carefully with anhydrous ethanol (3×20 mL) to remove organic species. The collected materials were left to dry in an oven at 60°C for 12 h and then calcined at different temperatures (100–400°C) for 2 h to obtain the MWCNT-TiO_2 hybrid nanostructures [11]. The samples contained 50 wt. % MWCNT in this paper.

2.4. Preparations of Nanofluids

In order to prepare the samples (MWCNT-TiO_2 nanofluids), a two-step process was used. MWCNT-TiO_2 with a wide range of concentrations (0.02, 0.04, 0.06 and 0.08% wt) was mixed up with a base fluid, i.e. distilled water, and placed in the ultrasonic

device (BANDELIN SONOPULS HD3200,140 W, 20 kHz, Figure 2) for 45 min [12].

Figure 2: *Ultrasonic device in laboratory*

2.5. Experimental setup and procedure

An experimental setup was developed to investigate the heat transfer coefficient of the nanofluid as shown in Figure 3 and 4.A commercial PHE manufactured by GEA Germany has was for this purpose. The geometric details of the plates and the heat exchanger are provided in Table 1 and Figure 5.

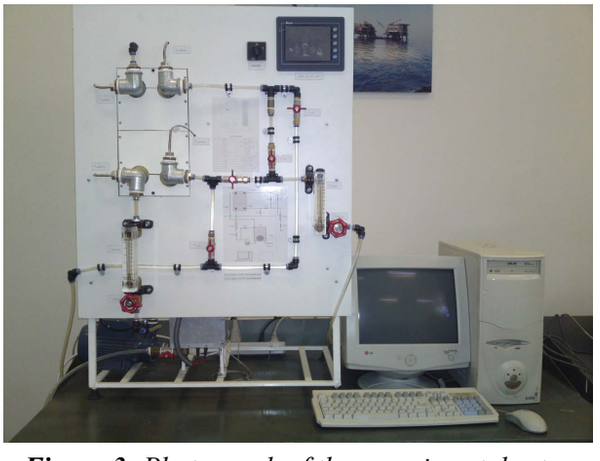

Figure 3: *Photograph of the experimental setup*

The experimental setup mainly included two flow loops, for the hot and cold fluids (nanofluid and water flow loops) as illustrated in Figure 4. The device consisted of a stainless steel tank, a heater, a pump, a plate heat exchanger, two gate valves, 5 on/off valves, 2 rotameters, 5 resistance thermocouples, PLC and a computer. The storage tank was made of stainless steel 304 to prevent corrosion and the tank size was 15×12×12 cm. To avoid heat loss, the tank was made of two layers of glass wool with some space between them. For heating the nanofluid a 2kW heater was built in the storage tank. Nanoparticles do not precipitate because of the mixing due to the fluid flow inside the exchanger.

Four RTD PT-100 probes measure the inlet and outlet temperatures of each stream. To control the flow rate of the nanofluid and cold water two rotameters were used. Flow rate of the Nnanofluid varied from 2 to 3.5 LPM whereas flow rate of the cold stream was 1 LPM in all tests. The minimum required nanofluid for the setup is 1100 ml.

A typical test normally lasted approximately 60 min. This time interval was required for the system to achieve steady-state conditions. In order to establish whether the system reached the steady-state conditions, the temperatures were constantly monitored.

Table 1: *Geometrical parameters of tested plate heat exchanger*

Vertical distance, H (cm)	282
Vertical distance between centers of ports, H_1 (cm)	239
Horizontal distance, W (cm)	127
Horizontal distance between centers of ports, W_1 (mm)	84
Port length, S (mm)	19.5
Operation Temperature, (^{0}C)	-196~204
maximum operation pressure, (bar)	33
Number of plates	6
Mean channel spacing, b_c (mm)	2.05
Plate thickness (mm)	0.6
Total area of heat transfer (m^2)	0.16

2.6. Data analysis

Experimental data was used to calculate the heat transfer coefficient of the nanofluids. Reynolds number of cold water can be calculated based on

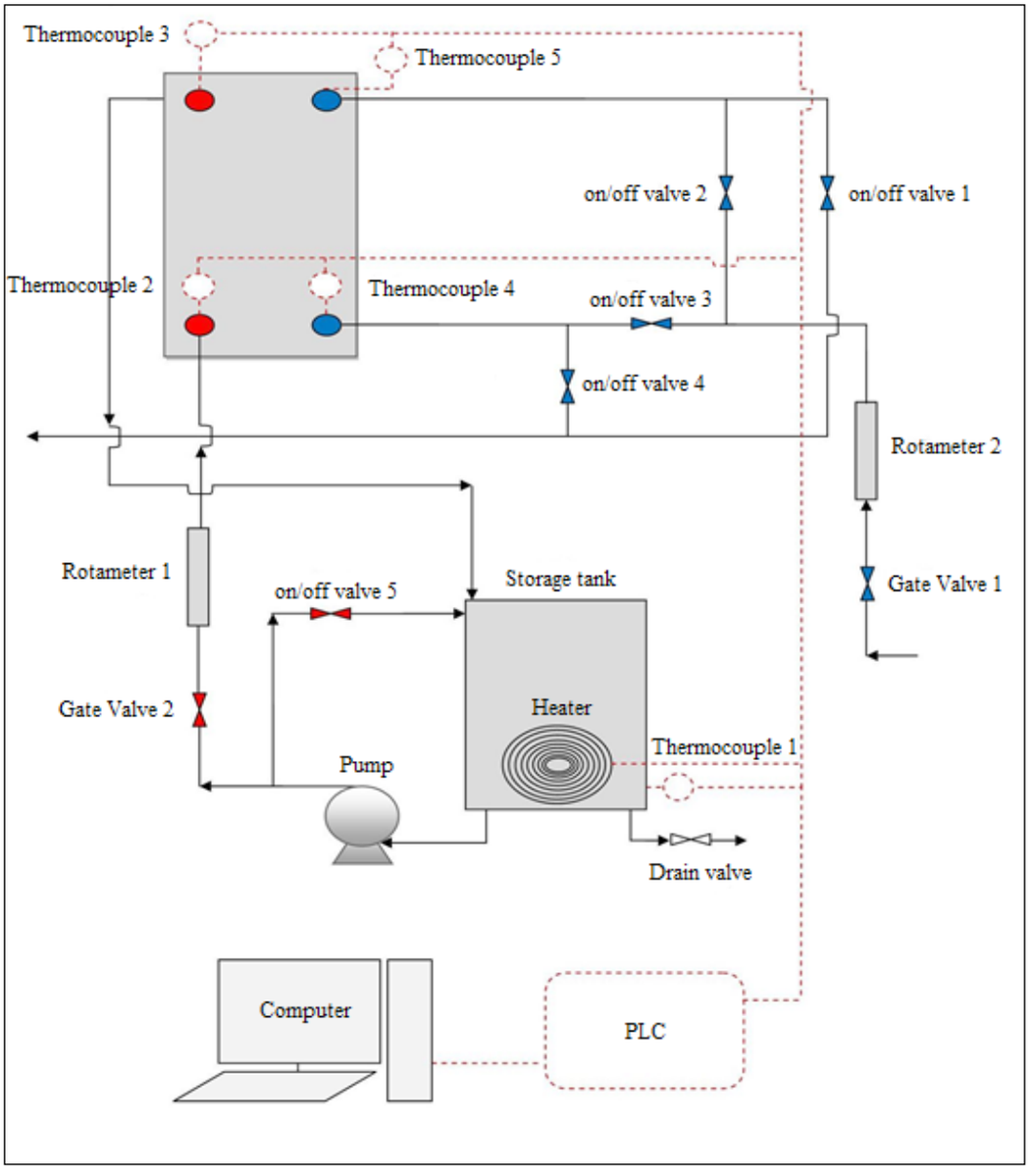

Figure 4: *Schematic diagram of the experimental setup*

channel mass velocity and hydraulic diameter of the channel as follows [13]:

$$\mathrm{Re}_w = \frac{G_w D_h}{\mu_w} \quad (1)$$

Where Dh=2bc is the hydraulic diameter. The channel mass velocity is obtained from the following relationship:

$$G_w = \dot{m}_w / n_{ch}.b_c.W \quad (2)$$

Where $n_{ch} = 3$ for cold and 2 for hot stream, respectively.

The heat has been removed by nanofluids and absorbed by the cold water, Q_c, is calculated by Eq. (3) using the measured temperature and mass-flow rate.

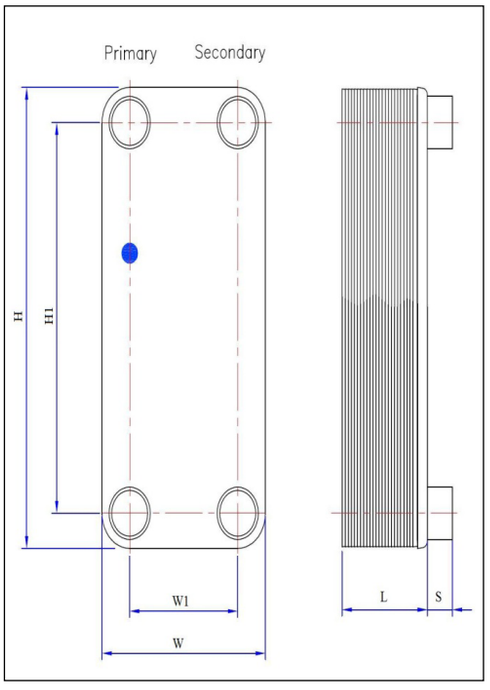

Figure 5: *Basic geometric parameters of plate heat exchanger*

$$Q_c = \dot{m}_c\, c_{p,c} \Delta T_c \tag{3}$$

The fluid properties are evaluated at bulk temperatures which are calculated as:

$$T_{b,c} = (T_{c,i} + T_{c,o}) / 2 \tag{4}$$

The Nusselt of the cold fluid can be calculated by the following equation [14]:

$$Nu_c = 0.455\, \mathrm{Re}_c^{\,0.66}\, \mathrm{Pr}_c^{\,0.33} \tag{5}$$

These values are obtained from the standardization on the water of the exchanger by the constructor.
The Prandtl number is defined as follows:

$$\mathrm{Pr}_c = \frac{\mu_c (C_p)_c}{k_c} \tag{6}$$

The heat transfer coefficient of water (cold stream) can be calculated by the following equation:

$$h_c = \frac{Nu_c . D_h}{k_c} \tag{7}$$

The overall heat transfer coefficient is calculated using Eq. (8) based on the experimental data:

$$U = \frac{Q_c}{A.F.\Delta T_{LMTD}} \tag{8}$$

Where A is the total heat transfer area of the PHE and F is the temperature correction factor, which can be taken equal to 1in the case of the countercurrent flow.

$$\Delta T_{LMTD} = \frac{\left(T_{\mathrm{nf},i} - T_{\mathrm{w},o}\right) - \left(T_{\mathrm{nf},o} - T_{\mathrm{w},i}\right)}{\ln\left(\left(T_{\mathrm{nf},i} - T_{\mathrm{w},o}\right) \Big/ \left(T_{\mathrm{nf},o} - T_{\mathrm{w},i}\right)\right)} \tag{9}$$

The heat transfer coefficient of nanofluids are evaluated using overall heat transfer coefficient and water heat transfer coefficient. Given the thermal conductivity of the plate, k, and its thickness, Δx, the heat transfer coefficient of nanofluids is obtained from the following relationship:

$$h_{nf} = \frac{1}{\left(\frac{1}{U} - \frac{1}{h_w} - \frac{\Delta x}{k}\right)} \tag{10}$$

3. RESULTS

3.1. FTIR spectroscopy

The functionalization & chemical structure of MWCNT were identified by FTIR (Thermo Scientific, Nicolet 6700). Typically 100 scans over the range 4000–500 cm^{-1} were taken from each sample with a resolution of 2 cm^{-1} and summed to provide the spectra. The results are shown in Figure 6.
The broad band of FTIR spectra between 3000 and 3700 cm^{-1} corresponds to the presence of the oxygenated groups [15]. The presence of carboxyl functional groups and OH groups could also be detected at around 1768 cm^{-1} and 3454 cm^{-1}, respectively[16]. The peaks at 1647 cm^{-1} and 1225 cm^{-1} can be attributed to C=C banding vibrations of aromatic structures and C-O banding, respectively [17].

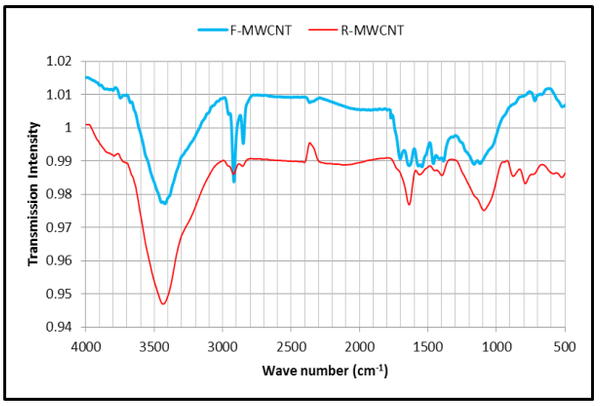

Figure 6: *FTIR of raw-MWCNT and func-MWCNT*

3.2. SEM imaging

The morphology of the TiO_2 on MWCNT was examined by SEM image. Scanning Electron Microscope (SEM) was carried out using KYKY-EM3200 at 40 kV. The SEM images of the functionalized MWCNT and MWCNT-TiO_2 hybrid are shown in Figure 7. As can be seen, the MWCNTs coated with well-dispersed TiO_2 particles are clearly shown, indicating that the MWCNTs and TiO_2 had an intimate contact.

3.3 XRD analysis

X-ray diffraction (XRD) patterns were analyzed by an X-ray diffractometer (Bruker AXS., Germany) using Cu Kα radiation source at 40 kV. The XRD patterns of the functionalized MWCNT and MWCNT-TiO_2 hybrid are shown in Figure 8
The XRD patterns reveal that only anatase phase of TiO_2 can be identified. The pristine MWCNTs have two typical diffraction peaks (002 and 101). For MWCNT-TiO_2 hybrid the main diffraction peaks of anatase TiO_2 (101, 004, 200, 105, 211, and 204) are clearly shown [9].

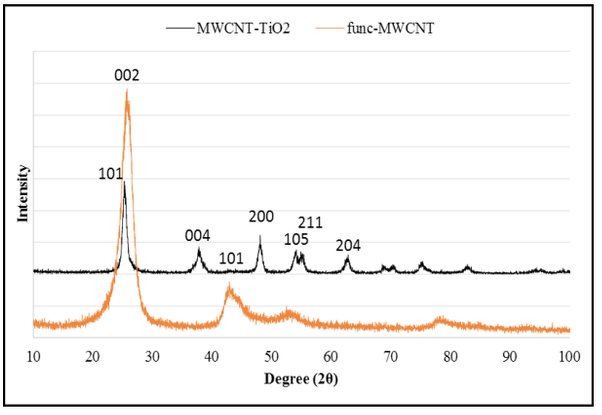

Figure 8: *XRD patterns of the func-MWCNT and MWCNT-TiO_2 hybrid*

Based on Scherrer equation the crystalline size of the anatase phases is 2.3 nm.

3.4. Heat transfer coefficient of nanofluid

To evaluate the reliability and accuracy of the measurements, experimental system was tested with distilled water before measuring the heat transfer of nanofluids. The results are shown in Figure 9.

a)

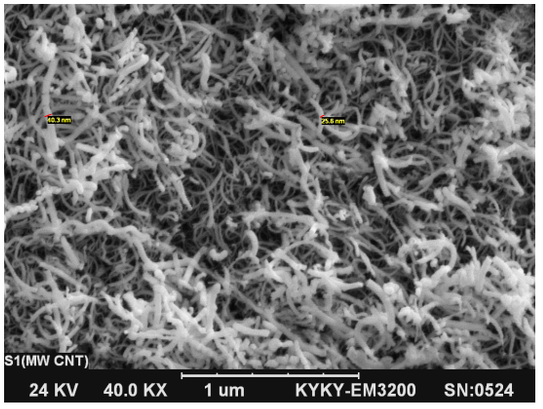

b)

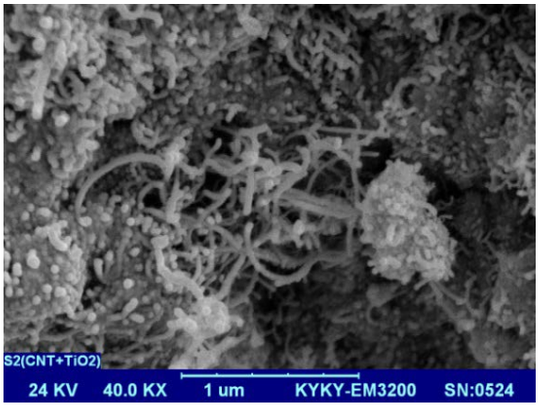

Figure 7: *SEM image of a) func-MWCNT, b) MWCNT-TiO_2 hybrid*

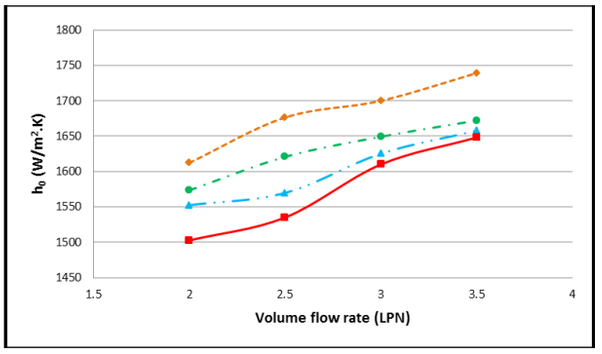

Figure 9: *Variation of heat transfer coefficient of distilled water nanofluid tested at different volume flow rates with various temperatures: a) 36^{0}C, b) 44^{o}C, c) 52^{o}C, d) 60^{o}C*

Figure 10 shows the variations of heat transfer coefficient of MWCNT-TiO_2 nanofluid with different weight concentrations (0.02, 0.04, 0.06 and 0.08 wt. %) in a wide range of volume flow rates (2, 2.5, 3 and 3.5 LPM) and at the flow rate of cold water equal to 1 LPM. As shown in Figure 10, the heat transfer coefficient increases with increasing w eight fraction of nanoparticles. Adding nanoparticles increases particle collisions and interactions. Nanoparticle penetration and relative motions near the wall plates may also increase the heat transfer.

Figure 11 shows the variations of the heat transfer coefficient ratio of MWCNT-TiO_2 nanofluid at different volume flow rates (2, 2.5, 3 and 3.5 LPM), different concentrations (0.02, 0.04, 0.06 and 0.08 wt. %) and at a flow rate of cold water equal to 1 LPM. At a constant inlet temperature and a particle weight concentration of nanoparticles, a higher flow rate of nanofluids causes a greater heat transfer coefficient ratio. As the flow rate of nanofluids increases, the influence of nanoparticle collision on the wall surface increases which leads to temperature rise. The outcome of this investigations

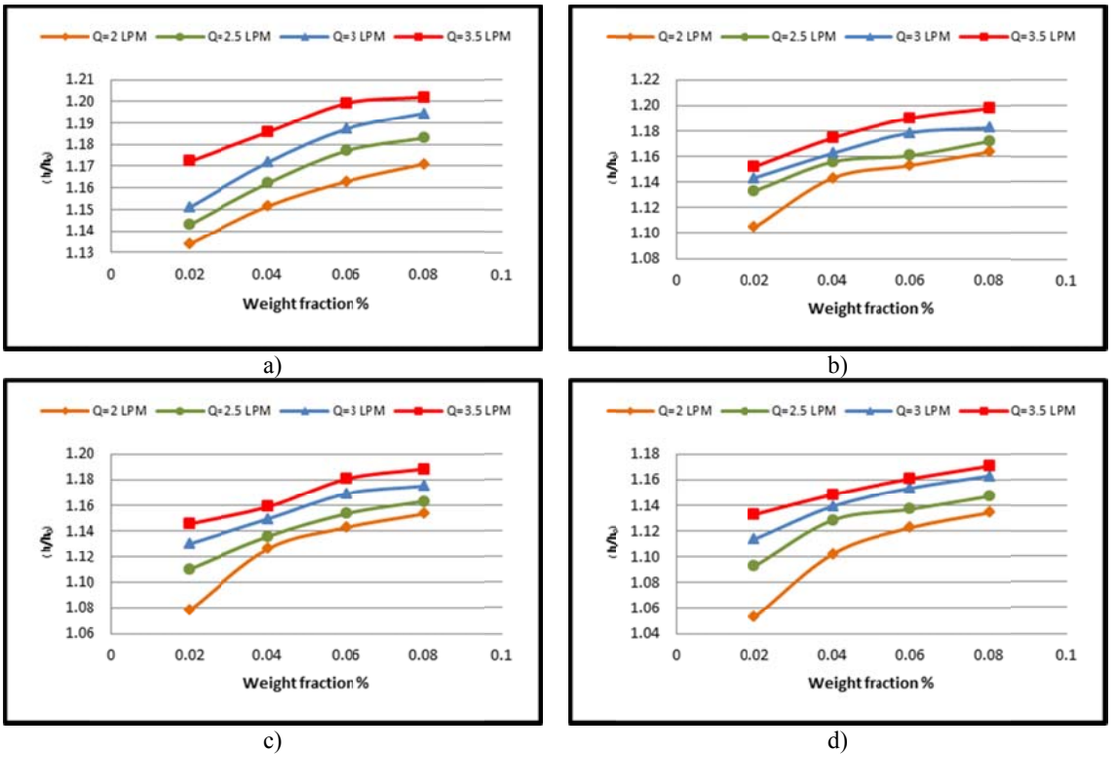

Figure 10: *Variation of heat transfer coefficient of MWCNT-TiO_2/water nanofluid tested at different weight concentrations with various temperatures: a) 36^{o}C, b) 44^{o}C, c) 52^{o}C, d) 60^{o}C*

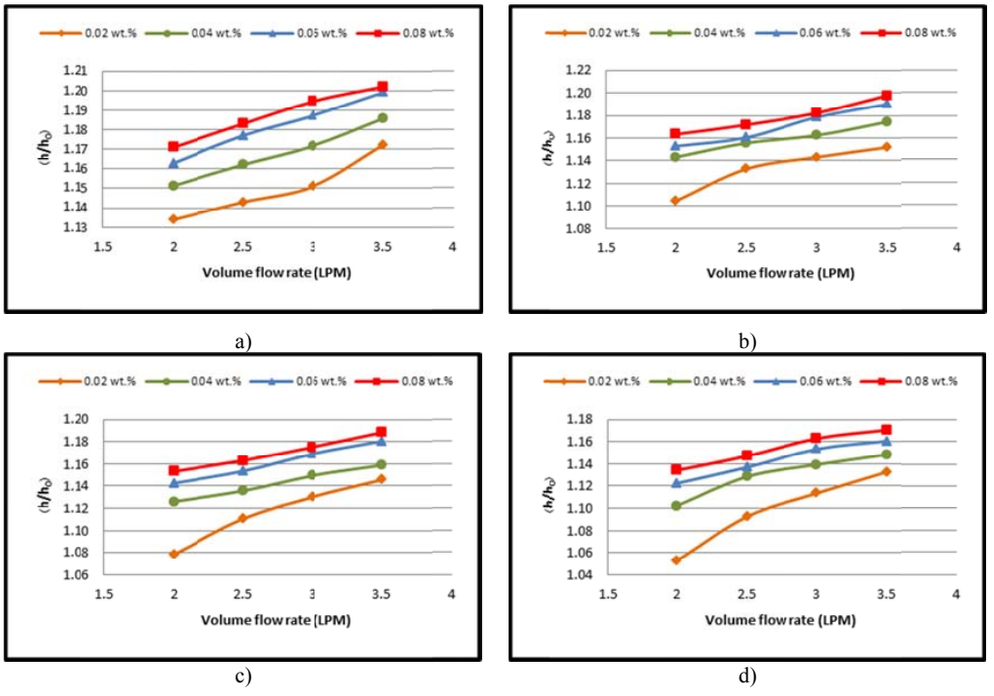

Figure 11: *Variation of heat transfer coefficient of MWCNT-TiO_2/water nano-fluid tested at different volume flow rates with various weight concentrations: a) 0.02 wt.%, b) 0.04 wt.%, c) 0.06 wt.%, d) 0.08 wt.%*

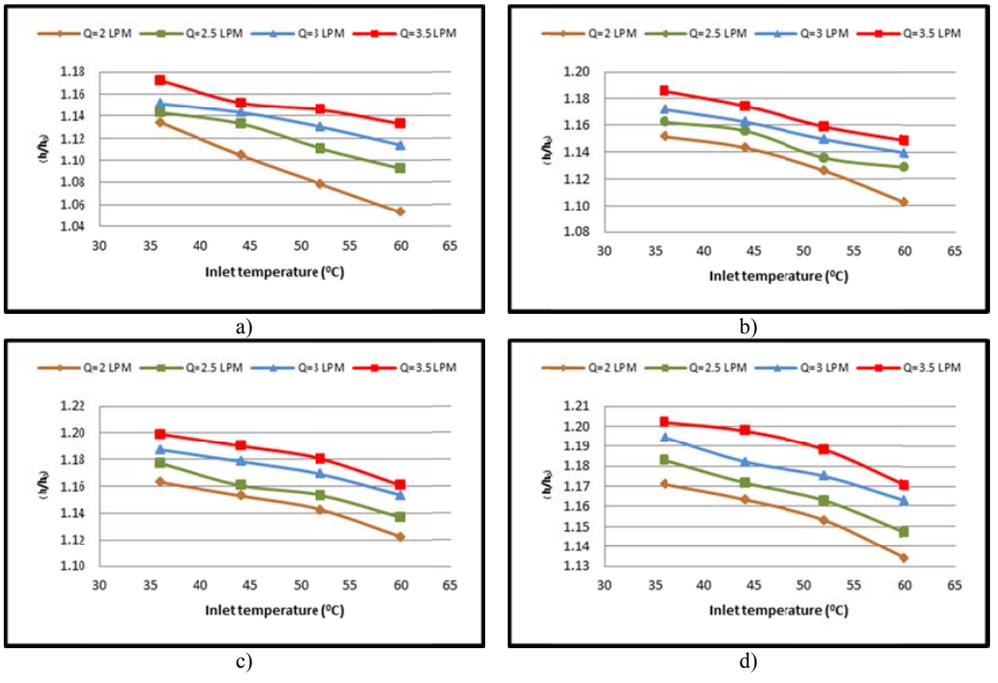

Figure 12: *Variation of heat transfer coefficient of MWCNT-TiO_2/water nano-fluid tested at different inlet temperatures with volume flow rates: a) 2 LPM b) 2.5 LPM, c) 3 LPM, d) 3.5 LPM*

showed that the heat transfer coefficient ratios of nanofluids increases significantly.

Figure 12 shows the variations of heat transfer coefficient of MWCNT-TiO_2 nanofluid at different temperatures (36, 44, 52 and 60°C) in a wide range of volume flow rates (2, 2.5, 3 and 3.5 LPM) and at a flow rate of cold water equal to 1 LPM. According to Figure 12, the ratio of the heat transfer coefficients (nanofluid to the base fluid) increases with decreasing the inlet temperature. The decrease in the heat transfer coefficient of the nanofluid with increasing the nanofluid inlet temperature can be due attributed to two factors [18]:

1. Rapid alignment of nanoparticles in lower viscosity fluids, leading to less contact between nanoparticles.
2. Depletion of particles in the near-wall fluid phase, leading to an intrinsically lower thermal conductivity layer at the wall.

4. CONCLUSION

In this paper, anatase TiO_2 nanoparticles were anchored on CNTs surface via solvothermal method and characterized by XRD, SEM and FT-IR techniques.

The heat transfer coefficient of a MWCNT-TiO_2 nanofluid flowing in a counter flow PHE was calculated. The experiments were done in a wide range of nanoparticle weight concentrations, flow rates and inlet temperatures of the nanofluid. The major conclusions are as follows:

The heat transfer coefficient decreased with increasing the inlet temperature of the nanofluid. At the temperatures of 44 and 60°C, the heat transfer coefficient of MWCNT-TiO_2 nanofluid enhanced 16.1% and 13.7% at 0.06 wt.% and 2 LPM compared with that of distilled water.

The heat transfer coefficient enhanced with the addition of nanoparticles to the base fluid. At the concentrations of 0.04 and 0.08 wt.% of MWCNT-TiO_2 nanoparticles, the heat transfer coefficient increased 18.6% and 20.2% compared with that of distilled water at 36°C and 3.5 LPM.

The heat transfer coefficient increased significantly with increasing the volumetric flow rate of the nanofluid. At the volume flow rates of 2.5 and 3 LPM of MWCNT-TiO_2 nanofluid, the heat transfer coefficient enhanced 11.1% and 13% at 0.02 wt.% and 52°C compared with that of distilled water.

ACKNOWLEDGEMENT

The authors wish to thank the Transport Phenomena and Nanotechnology Laboratory (TPNT) for their great support to this project.

ABBREVIATIONS

MWCNT:	multi wall carbon nano tube
XRD :	X-ray diffraction
SEM :	scanning electron microscopy
PHE :	plate heat exchanger
LPM:	litter per minute

REFERENCE

1. S.U.S. Choi, Developments Applications of Non-Newtonian Flows, Vol. 1, (1995), pp.99-105.
2. A. K. Tiwari, P. Ghosh, and J. Sarkar, Experimental Thermal and Fluid Science, Vol.49, (2013), pp.141-151.
3. B. R. Lazarus Godson, D. Mohan Lal, and S. Wongwises, Renewable and Sustainable Energy Reviews, Vol.1, (2010), pp.641-629.
4. S. K. a. A. Pramuanjaroenkij, Heat and Mass Transfer, Vol. 52, (2009), pp.3187–3196,.
5. J. Sarkar, Renewable and Sustainable Energy Reviews, Vol. 15, (2011), pp.3271-3277.
6. A. S. M. X.-Q. Wang, a review, Vol. 3, (2007), pp. 1–19.
7. L. G. Yao Y, Ciston S, Lueptow RM, Gray KA, Environ Sci Technol, Vol. 42, (2008), pp. 7-13.
8. D. Eder, Materials Science and Metallurgy, Vol. 2, (2010), pp. 15-27.
9. X. Yan, D. Pan, Z. Li, B. Zhao, J. Zhang, and M. Wu, Materials Letters, Vol. 64, (2010), pp.1694-1697.
10. A. D. M. Goran D. Vukovi, Sreco D. Skapin, Mirjana Đ. Risti, Aleksandra A. Peri c-Gruji, Petar S.

Uskokovi , Radoslav Aleksi, Chemical Engineering, Vol. 173, (2011), pp. -23.

11. L. Tian, L. Ye, K. Deng, and L. Zan, Solid State Chemistry, Vol. 184, (2011), pp. 1465-1471.
12. L. Zhang, Q. Ni, Y. Fu, T. Natsuki, Appl. Surf. Sci,Vol. 255, No. 15, (2009), pp. 7095–7099.
13. B.R. Munson, D.F. Young, T.H. Okiishi, (2002), 4ed, John Wiley & Sons Inc, New York, pp. 41-70.
14. J.H. Lienhard IV, A Heat Transfer Textbook, second ed., Phlogiston Press, (2002).
15. A.J. L.P.C. Hontoria-Lucas, J.de D. López-González, M.L. Rojas-Cervantes, and R.M. Martín-Aranda, Study, Carbon,Vol. 3, (1995), pp. 132-141.
16. S. W. D. Pan, B. Zhao, M. Wu, H. Zhang, Y. Wang, Z. Jiao, Li, Chemistry of Materials, Vol. 21, (2009), pp.7-15.
17. K. M. Sankaran Murugesan, Vaidyanathan (Ravi) Subramanian, Applied Catalysis B: Environmental, Vol.103, (2011), pp. 9-18.
18. M. Naraki, S. M. Peyghambarzadeh, S. H. Hashemabadi, and Y. Vermahmoudi, Thermal Sciences, Vol. 66, (2013), pp. 82-90.